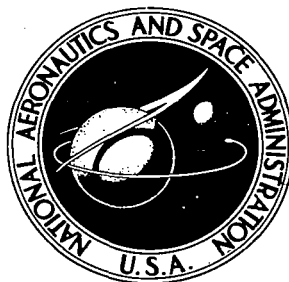


NASA TECHNICAL NOTE



NASA TN D-6867

NASA TN D-6867



GROUND AND FLIGHT TEST METHODS
FOR DETERMINING LIMIT CYCLE
AND STRUCTURAL RESONANCE
CHARACTERISTICS OF AIRCRAFT
STABILITY AUGMENTATION SYSTEMS

by Weneth D. Painter and George J. Sitterle

*Flight Research Center
Edwards, Calif. 93523*





0133728

1. Report No. NASA TN D-6867		2. Government Accession No.		3. Recipient's Catalog No.	
4. Title and Subtitle GROUND AND FLIGHT TEST METHODS FOR DETERMINING LIMIT CYCLE AND STRUCTURAL RESONANCE CHARACTERISTICS OF AIR-CRAFT STABILITY AUGMENTATION SYSTEMS				5. Report Date June 1972	
				6. Performing Organization Code	
7. Author(s) Weneth D. Painter and George J. Sitterle				8. Performing Organization Report No. H-682	
9. Performing Organization Name and Address NASA Flight Research Center P. O. Box 273 Edwards, California 93523				10. Work Unit No. 136-62-01-00-24	
				11. Contract or Grant No.	
12. Sponsoring Agency Name and Address National Aeronautics and Space Administration Washington, D. C. 20546				13. Type of Report and Period Covered Technical Note	
				14. Sponsoring Agency Code	
15. Supplementary Notes					
16. Abstract <p>Performance criteria and test techniques are applied to stability augmentation systems (SAS) during ground testing to predict objectionable limit cycles and preclude structural resonance during flight. Factors that give rise to these problems, means of suppressing their effects, trade-offs to be considered, and ground test methods that have been developed are discussed in detail. SAS performance predicted on the basis of these tests is compared with flight data obtained from three lifting body vehicles and the X-15 research airplane. Limit cycle and structural resonance test criteria, based upon ground and flight experience and data, were successfully applied to these vehicles. The criteria used were: The limit cycle amplitude (SAS gain multiplied by peak-to-peak angular rate) shall not exceed 0.5° for the highest product of control power and SAS gain that will be used in flight; the maximum in-flight SAS gain should never exceed 50 percent of the value at which a structural resonance can be sustained during ground test.</p>					
17. Key Words (Suggested by Author(s)) Stability augmentation systems Limit cycle Structural resonance			18. Distribution Statement Unclassified - Unlimited		
19. Security Classif. (of this report) Unclassified		20. Security Classif. (of this page) Unclassified		21. No. of Pages 20	22. Price* \$3.00

GROUND AND FLIGHT TEST METHODS FOR DETERMINING LIMIT CYCLE AND STRUCTURAL RESONANCE CHARACTERISTICS OF AIRCRAFT

STABILITY AUGMENTATION SYSTEMS

Weneth D. Painter and George J. Sitterle
Flight Research Center

INTRODUCTION

Stability augmentation systems (SAS) are necessary on most high-performance aircraft to achieve satisfactory vehicle control over a broad range of flight conditions. For optimum performance, some of these systems require multiple sensors, complicated automatic gain scheduling, and shaping networks. Thus the use of stability augmentation systems can give rise to a number of problems, including limit cycle and structural resonance. Because these systems are for high-performance, advanced vehicles, documentation of the associated problems is limited; references 1 to 8 present some of the available information.

In order to avoid flight problems, such as limit cycle and structural resonance, SAS ground tests are usually performed prior to flight. However, if ground testing techniques are inadequate, an in-flight limit cycle or structural resonance can be severe enough to have catastrophic consequences.

This paper reviews flight experience with limit cycle and structural resonance problems at the NASA Flight Research Center and describes ground test techniques that were used to predict objectionable limit cycles and preclude structural resonance in flight. Test criteria are established for use during the initial flight testing of aircraft with high-gain stability augmentation systems. Ground test results are compared with flight test data obtained from three lifting body vehicles and the X-15 research airplane (refs. 1, 2, 4, 6, and 8).

SYMBOLS

Physical quantities in this report are given in the International System of Units (SI) and parenthetically in U. S. Customary Units. Measurements were taken in Customary Units. Factors relating the two systems are presented in reference 9.

$ A $	absolute value of normalized amplitude ratio, $\frac{\text{Surface deflection}}{\text{Angular rate}}$
b	reference wing span, m (ft)
C_{l_p}	roll-damping coefficient, per rad
$C_{l_{\delta_a}}$	rolling-moment coefficient due to aileron deflection, per deg

C_{m_q}	pitch-damping coefficient, per rad
$C_{m_{\delta_e}}$	pitching-moment coefficient due to elevon deflection, per deg
C_{n_r}	yaw-damping coefficient, per rad
$C_{n_{\delta_r}}$	yawing-moment coefficient due to rudder deflection, per deg
\bar{c}	reference chord, m (ft)
f	frequency, Hz
f_{BW}	system frequency bandwidth, Hz
I_{XX}	moment of inertia of the airplane about the X-axis, kg-m^2 (slug-ft ²)
I_{YY}	moment of inertia of the airplane about the Y-axis, kg-m^2 (slug-ft ²)
I_{ZZ}	moment of inertia of the airplane about the Z-axis, kg-m^2 (slug-ft ²)
K_p	roll-damper gain, deg/deg/sec
K_q	pitch-damper gain, deg/deg/sec
K_r	yaw-damper gain, deg/deg/sec
L_p	roll damping, $\text{rad/sec}^2/\text{rad/sec}$
L_{p_t}	roll damping with SAS, $\text{rad/sec}^2/\text{rad/sec}$
L_{δ_a}	roll control effectiveness, $\frac{\text{Moment per } \delta_a}{I_{XX}}$, $\text{rad/sec}^2/\text{rad}$ (referred to herein as roll control power)
M_q	pitch damping, $\text{rad/sec}^2/\text{rad/sec}$
M_{q_t}	pitch damping with SAS, $\text{rad/sec}^2/\text{rad/sec}$
M_{δ_e}	pitch control effectiveness, $\frac{\text{Moment per } \delta_e}{I_{YY}}$, $\text{rad/sec}^2/\text{rad}$ (referred to herein as pitch control power)

N_r	yaw damping, rad/sec ² /rad/sec
N_{r_t}	yaw damping with SAS, rad/sec ² /rad/sec
N_{δ_r}	yaw control effectiveness, $\frac{\text{Moment per } \delta_r}{I_{ZZ}}$, rad/sec ² /rad (referred to herein as yaw control power)
p	roll rate, deg/sec
q	pitch rate, deg/sec
\bar{q}	dynamic pressure, N/m ² (lb/ft ²)
Δq	steady-state pitch rate limit cycle amplitude, peak to peak, deg/sec
r	yaw rate, deg/sec
S	reference wing area, m ² (ft ²)
s	Laplace variable
$T_{1/2}$	time to damp to one-half amplitude, sec
t	time, sec
V	velocity, m/sec (ft/sec)
δ_a	"aileron" or total differential surface deflection, deg
δ_e	"elevator" or average horizontal-stabilizer deflection, deg
δ_r	rudder deflection, deg
ζ	damping ratio
ω_n	undamped natural frequency, rad/sec

DESCRIPTION OF A TYPICAL STABILITY AUGMENTATION SYSTEM

A functional diagram of a typical stability augmentation system is shown in figure 1. The essential components of the system are a rate gyro, a SAS gain selector, amplification and shaping, and a SAS servo. The output of a SAS servo goes to a control surface, possibly through a larger power actuator connected directly to the control surface.

A SAS provides damping inputs to aerodynamic control surfaces by sensing vehicle motion with rate gyros and using these signals to drive the control surfaces to provide

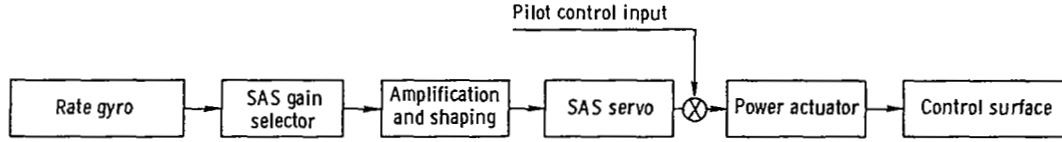


Figure 1. Functional diagram of typical SAS used in analysis.

additional damping. The rate gyro output signals are conditioned, shaped, filtered, amplified, and then used for servo commands to the servoactuators.

Artificial damping provided by a SAS is a function of control power and system gain in the rate feedback loop. The difference between the approximated moment equations with and without SAS is the effect of the SAS, as shown in the following table:

	Without SAS	With SAS
Pitch	$M_q = \frac{\bar{q}S\bar{c}^2 C_{m_q}}{2VI_{YY}}$	$M_{q_t} = \frac{\bar{q}S\bar{c}^2 \left(C_{m_q} + \frac{2VK_q}{\bar{c}} C_{m_{\delta_e}} \right)}{2VI_{YY}}$
Roll	$L_p = \frac{\bar{q}Sb^2 C_{l_p}}{2VI_{XX}}$	$L_{p_t} = \frac{\bar{q}Sb^2 \left(C_{l_p} + \frac{2VK_p}{b} C_{l_{\delta_a}} \right)}{2VI_{XX}}$
Yaw	$N_r = \frac{\bar{q}Sb^2 C_{n_r}}{2VI_{ZZ}}$	$N_{r_t} = \frac{\bar{q}Sb^2 \left(C_{n_r} + \frac{2VK_r}{b} C_{n_{\delta_r}} \right)}{2VI_{ZZ}}$

The equations in which SAS is included can be rewritten as:

$$\text{Pitch: } M_{q_t} = M_q + K_q M_{\delta_e}$$

$$\text{Roll: } L_{p_t} = L_p + K_p L_{\delta_a}$$

$$\text{Yaw: } N_{r_t} = N_r + K_r N_{\delta_r}$$

where K_q , K_p , and K_r represent SAS gain and M_{δ_e} , L_{δ_a} , and N_{δ_r} represent control power.

Sources of Instability

The performance of a stability augmentation system in an aircraft is influenced by many factors, such as attainable tolerances and hardware manufacturing techniques. Vehicle structural rigidity, mechanical control system nonlinearities due to hysteresis, friction and backlash, and electronic system noise and sensitivity are some of the characteristics that are manifested in two primary problems: limit cycle and structural resonance.

Limit cycle phenomenon.—With a fixed input, SAS gain, and vehicle control power, the output of the damping control surface may oscillate with a fixed amplitude and frequency. This condition is referred to as a limit cycle oscillation. It is reached only when the closed-loop phase lag is precisely 180° and is caused primarily by considerable hysteresis due to the accumulated free play of the large number of mechanical linkages in the control system and the nonlinearities in the surface power actuators.

Structural resonance phenomenon.—Sustained vibrations caused by stability augmentation systems have been encountered on many high-performance vehicles, such as the M2-F2, HL-10, and X-24A lifting bodies and the X-15 airplane (ref. 2). One explanation of this phenomenon is that a shock to a surface creates a ringing effect which causes the relatively rigid but freely supported vehicle to oscillate at a small but perceptible amplitude. This motion is sensed by the SAS rate gyros, and signals are sent to the servos to damp the motion. However, the accumulated phase lag at these frequencies is large and the SAS input only serves to sustain the vibration.

Importance of Nonlinearities

Conceivably, a system could be designed to operate essentially linearly for all expected inputs, but such a design would probably not be economically feasible. For example, the rating of power sources, and the amplifiers and precision mechanical linkages required for such a design would be prohibitive because of space, weight, manufacturing, and cost considerations. Fortunately, a design of this type is not usually required and may not be optimum even if achieved. Linear operation is normally necessary only for small deviations about the operating point. For large deviations, rate limiting and saturation of power sources are often acceptable in single-driven axes. However, for large deviations the change in system operating characteristics must not result in unsatisfactory performance when the system is synchronizing on the new operating point.

For small deviations, the nonlinearities which cause deadband, hysteresis, and signal distortion must be minimized. Again, it is usually not practical to eliminate the cause. The location of the sensors and SAS servos should be a primary consideration in the design of a stability augmentation system. However, those nonlinearities which are important at low signal levels can cause a self-sustained oscillation of low amplitude. The amplitude and frequency of these oscillations must not be large enough to affect system performance adversely.

GROUND TESTING

Flight stability augmentation systems usually are subjected to detailed and integrated checkout tests on the ground prior to flight use. Vehicle and SAS ground tests at the NASA Flight Research Center fall into four major categories: system calibration, frequency response, limit cycle, and structural resonance. In general, these tests are conducted in a hangar with the actual vehicle and flight hardware, using the ground electrical and hydraulic power supplies. Ground test and recording equipment is placed adjacent to the vehicle for convenience.

System Calibration

The system calibration test documents the steady-state characteristics of the SAS as well as the SAS components. The primary test equipment used is an angular rate table, an ac/dc voltmeter, and a direct reading recorder.

The rate gyros are removed from the vehicle and placed on a rate table, which is used for inertial torquing at controlled angular rates. Gyro characteristics in terms of range (maximum rate which gyros can sense) and voltage gradient (output measured with the ac/dc voltmeter in terms of volts per deg per sec) are determined. The inertial torquing rates are measured clockwise and counterclockwise. The gyros are checked for cross talk (for example, a yaw gyro sensing roll rate due to unwanted gyro tilt).

The SAS gain control is calibrated in terms of degrees/degrees/second. Both the gyro rate and the control surface position are recorded in order to compute the value of steady-state gains. The SAS control surface authorities are measured in degrees of maximum deflection.

The follow-up voltage of the SAS servo is calibrated in terms of volts per inch of SAS servo travel. These calibrations are compared with design values in order to determine the correct SAS gain control position for the desired stability of the vehicle and the maximum gain position at which limit cycle and structural resonance will occur.

Frequency Response

The frequency response test documents the open-loop dynamic characteristics of the SAS from rate gyro to control surface. This test is important because it can show dynamic gain and possible areas that could cause a structural resonance, a limit cycle, or other system instability. A function generator, an oscillating table, a direct-reading recorder, and a frequency analyzer are required. The test is performed at control surface amplitudes of 0.25°, 0.5°, 1.0°, and 50-percent peak-to-peak SAS surface authority and over a meaningful range of frequencies, possibly 0.01 hertz to 30 hertz. Time histories of the input to the rate gyros and the output of the servoactuator and control surface are recorded. The frequency response data are plotted in the form of a Bode plot. A typical example is shown in figure 2 for the pitch axis of the X-24A lifting body. The SAS bandwidth is then defined at the frequency for which the phase lag is 90°. The required system frequency bandwidth, f_{BW} , can be determined from the following relationships for the pitch axis:

$$f_{BW} \approx \frac{K_q M_{\delta_e} |A|}{2\pi} \text{ in hertz}$$

where $|A|$ is the absolute amplitude ratio of $\frac{\delta_e}{q}$ at the 90° phase-lag frequency and

$$M_{\delta_e} = \frac{S\bar{c}\bar{q}}{I_{YY}} C_{m_{\delta_e}} \text{ per sec}^2$$

The value of M_{δ_e} used in the frequency bandwidth calculations is the maximum value obtained from a plot such as that of figure 3.

Limit Cycle

Closed-loop test. - The ground test to determine limit cycle characteristics requires the use of an analog computer to simulate the aircraft response to surface motion. The limit cycle characteristics are strongly dependent on flight conditions and, specifically, control power. A simplified transfer function is used to relate aircraft rate to surface deflection, as follows:

$$\text{Pitch } \frac{q(s)}{\delta_e(s)} = \frac{M_{\delta_e}}{s}$$

$$\text{Roll } \frac{p(s)}{\delta_a(s)} = \frac{L_{\delta_a}}{s}$$

$$\text{Yaw } \frac{r(s)}{\delta_r(s)} = \frac{N_{\delta_r}}{s}$$

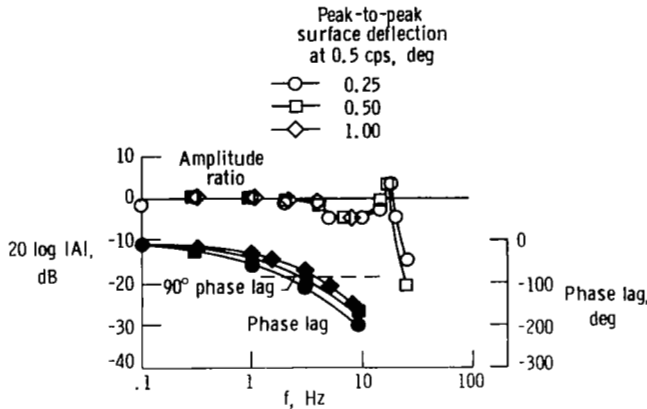


Figure 2. Frequency response of the pitch SAS of the X-24A lifting body. Gyro to control surface.

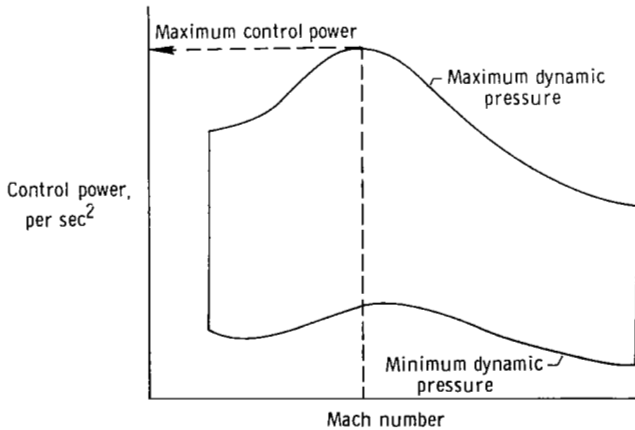


Figure 3. Typical vehicle flight envelope for analysis of limit cycle characteristics.

The division by the complex variable s is an integration process in the time domain and indicates that the output angular velocity lags the input surface deflection by 90° . Because a phase lag of 180° and a loop gain of unity are necessary conditions for a limit

cycle oscillation, the remaining 90° of phase lag is from the SAS electronics, mechanical system, power actuators, or filters.

The analog computer setup shown in figure 4 simulates the vehicle aerodynamics and permits closed-loop testing for limit cycles. Values of the measured surface deflection are obtained from transducers on the actual control surface and are used as inputs to the computer. By using the control surface motion, the vehicle response is computed for values of control power and SAS gain. A signal that represents the vehicle angular rate can then be fed back to the control system.

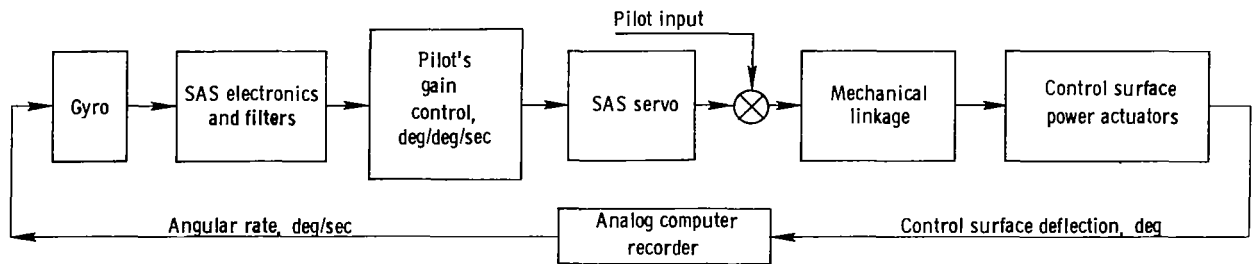


Figure 4. Limit cycle test setup.

When possible, the signal of the computed rate is used to torque the aircraft gyro. When this is not practical, the computed rate signal is passed through a simulated gyro transfer function and introduced into the aircraft's control system immediately downstream of the gyro.

The computer is used to alter the total loop gain (SAS gain multiplied by control power). At each gain condition, a small disturbance is introduced into the system. Surface positions and computed rates are recorded to determine the frequency and amplitude of the steady-state limit cycle. Figure 5, a time history of a limit cycle test on the HL-10 roll SAS, shows the angular rate and control surface deflection. It should be pointed out that $K_q \Delta q$, the product of peak-to-peak vehicle angular rate and SAS gain, is used as a measure of limit cycle amplitude. In figure 6 the quantity K_q is included in the ordinate of the left-hand plot to offset the effect of K_q in the abscissa; thus, the plot is a representation of vehicle motion as a function of control power.

The total loop gain is increased until the system is driven unstable. Large amplitude limit cycles on the ground can damage an aircraft; therefore, the system must be disengaged when a divergence is observed. In figure 6 the resulting values of limit cycle amplitude (peak-to-peak angular rate multiplied by SAS gain) and frequency are plotted against the total loop gain (SAS gain multiplied by control power) for the pitch SAS of the X-24A vehicle.

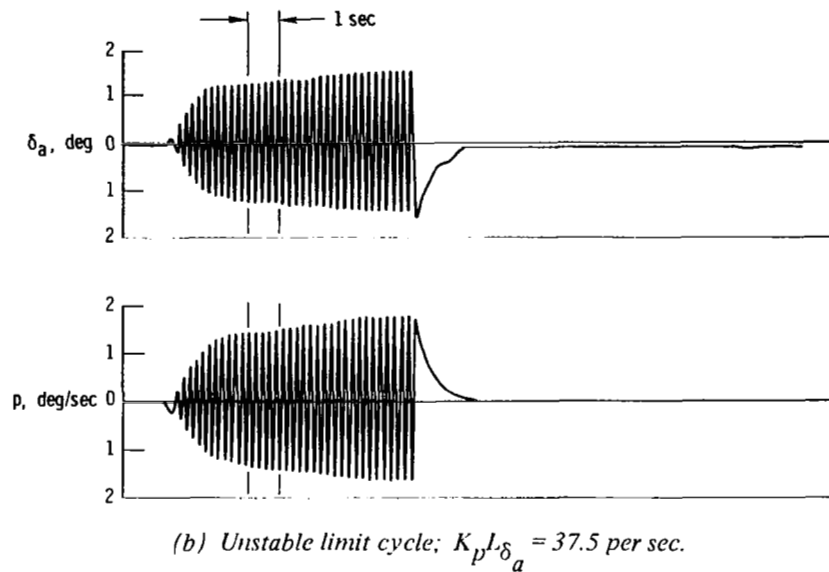
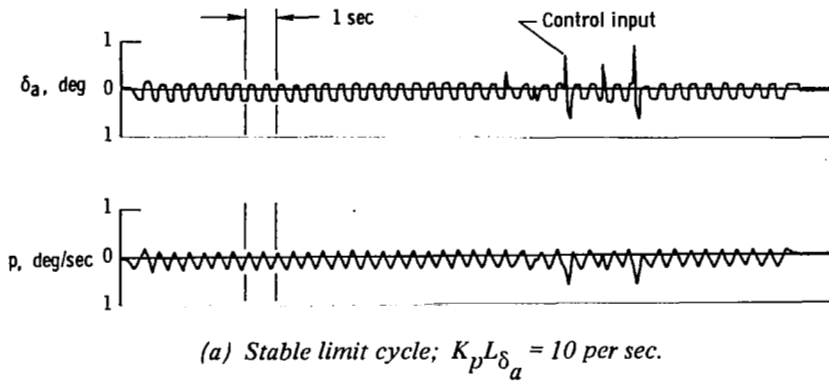


Figure 5. Time histories of limit cycle ground test characteristics of the roll SAS of the HL-10 lifting body.

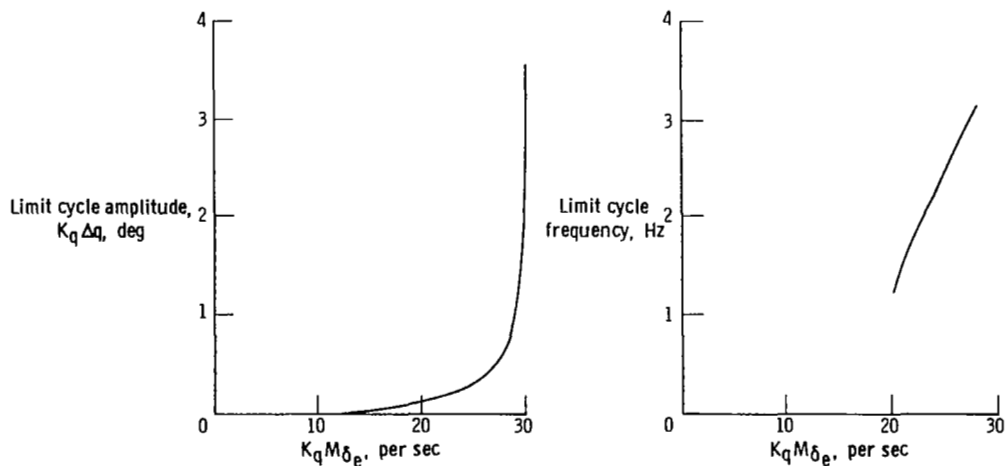


Figure 6. Typical limit cycle ground test characteristics of the pitch SAS of the X-24A lifting body.

Figure 7 illustrates the limit cycle characteristics at various points in the HL-10 SAS. The accumulated phase lags from the electronics are small, and the system can

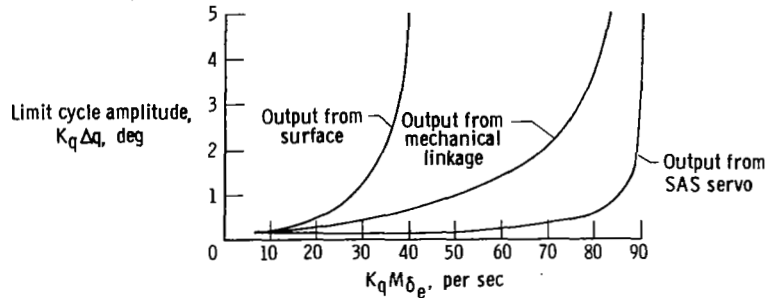


Figure 7. Typical limit cycle ground test characteristics of the pitch SAS of the HL-10 lifting body at various points within the system.

be operated at extremely high loop gains when the power actuator and linkages to the SAS servo are neglected. The additional phase lags due to the mechanical linkages and power actuator cause a significant reduction in the total loop gain at which the system can be operated. Thus the position transducer must be located on the actual control surface for the limit cycle test.

Figure 8 shows the limit cycle damping ratio as a function of control power during a ground test in which the analog computer was used to close the loop. Damping of the

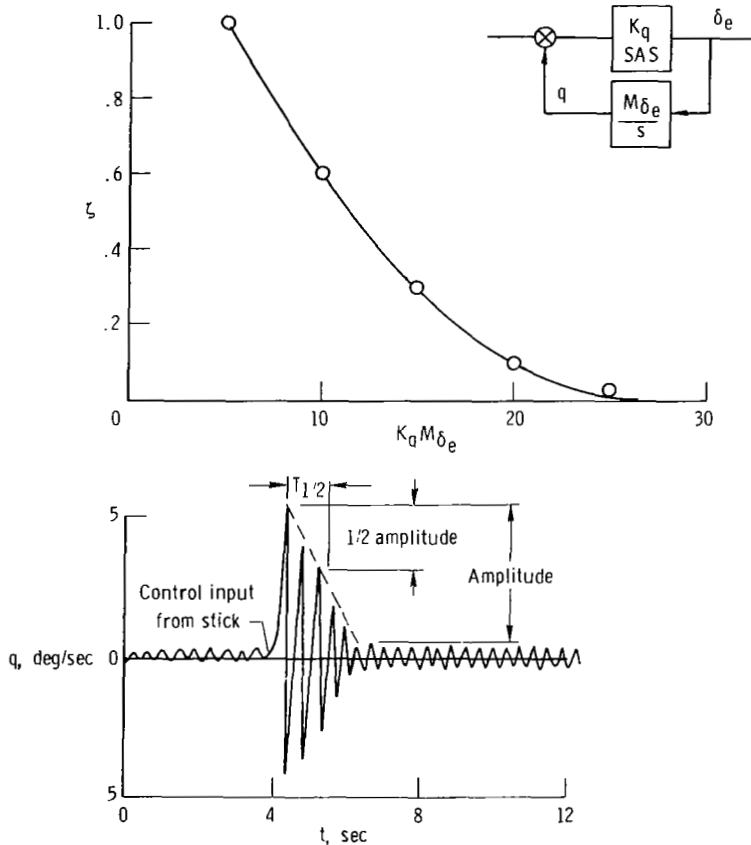


Figure 8. Damping of limit cycle characteristics of the pitch SAS of the M2-F2 lifting body.

limit cycle decreases as the control power increases. The damping ratio is computed by using the time-to-damp-to-one-half-amplitude after a control input is introduced into

the system. The equations used are $T_{1/2} = \frac{0.69}{\zeta \omega_n}$, $\zeta = \frac{0.69}{\omega_n T_{1/2}}$.

Open-loop test.—Although not as accurate as the analog computer method, the Bode plot method is another means of determining limit cycle characteristics. An open-loop frequency response test is conducted on the system from the SAS gyro to the control surface. The test data are presented in a Bode plot, as illustrated in figure 9. The point at which a 90° phase lag occurs provides the limit cycle amplitude and frequency.

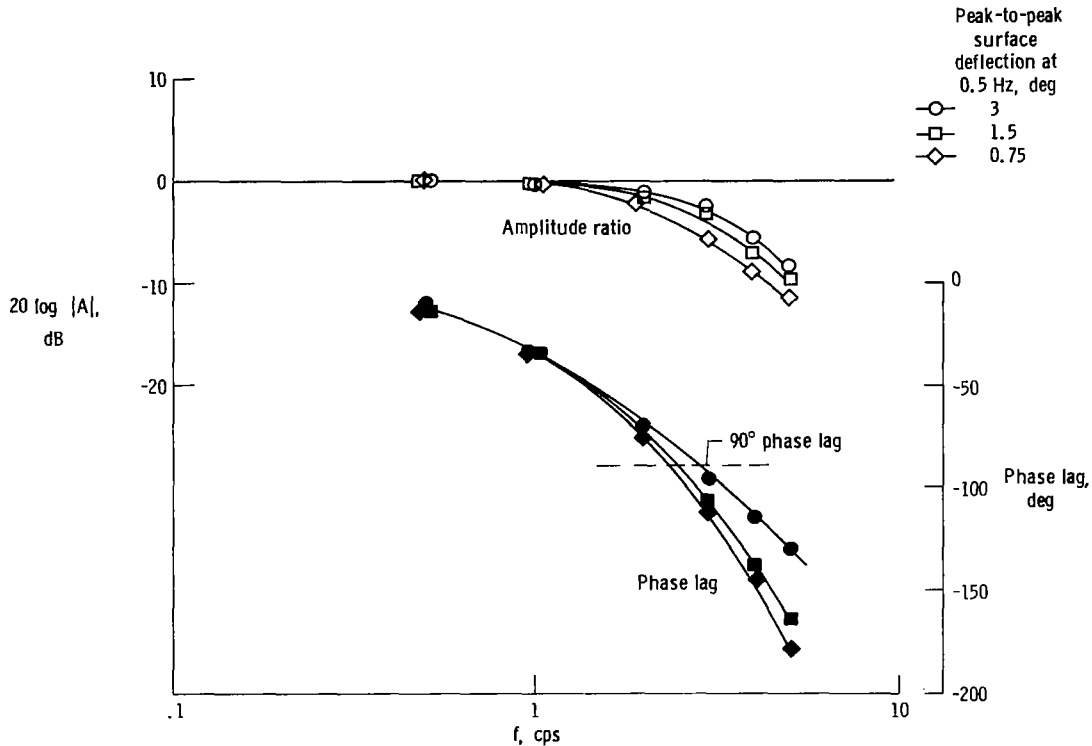


Figure 9. Frequency response of the pitch SAS of the M2-F2 lifting body. Gyro to control surface.

A limit cycle characteristics curve can then be plotted, using the following equation:

$$K_q M \delta_e \approx \frac{2\pi f(-90^\circ)}{|A|}$$

This equation represents a phase lag of approximately 90° for a closed-loop system which includes the vehicle. Figure 10 compares the limit cycle characteristics of the M2-F2 lifting body obtained by using the Bode plot (open loop) and the analog computer (closed loop) methods.

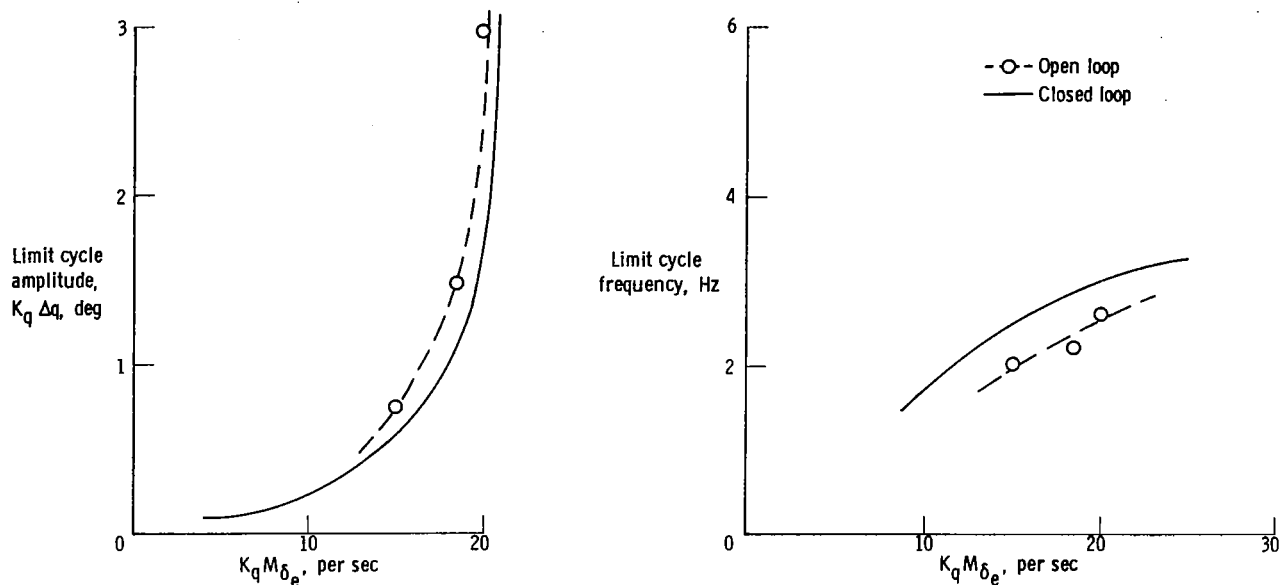


Figure 10. Comparison of limit cycle characteristics determined by the Bode plot and analog computer methods for the M2-F2 lifting body.

Structural Resonance

The ground test for structural resonance sometimes requires a means of artificially increasing the gain in each axis of the sensor feedback loops above the normal flight values. The structural resonance problem for the worst case is assumed to be independent of the vehicle flight conditions; therefore, no aerodynamic closed-loop computation is required (no integration). While the tests are being performed, the vehicle configuration is as close to the flight configuration as possible. Instrumentation is used to record control surface position, gyro output, SAS servo position, or any other quantity that might be helpful in measuring amplitudes and frequencies. The gains in each feedback loop (one axis at a time) are varied over the available range, which should considerably exceed the maximum possible flight value. Figure 11 shows the results of a ground test performed on the SAS of the X-24A lifting body.

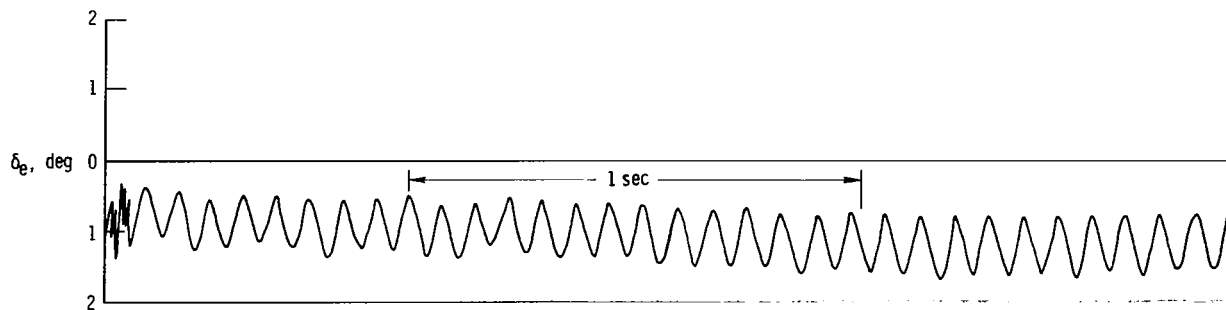


Figure 11. Ground test measurement of structural resonance in the pitch SAS of the X-24A lifting body.

If resonance-free operation cannot be achieved at the desired gain levels, the flight

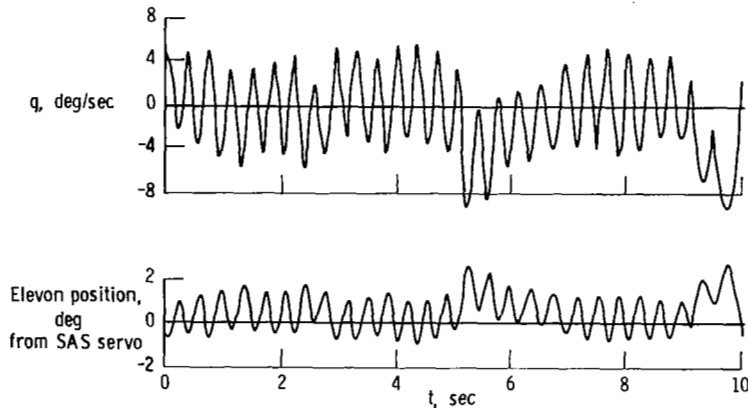
control system is modified to reduce the gain at the particular frequency that was excited, the structure is strengthened to increase its natural resonant frequency, or the sensor is relocated.

When ground tests are completed, the data are reviewed to estimate the severity of the resonance that occurred during the test. If the severity is significant, the vehicle's structure and control system linkage are thoroughly inspected before flight to assess possible damage.

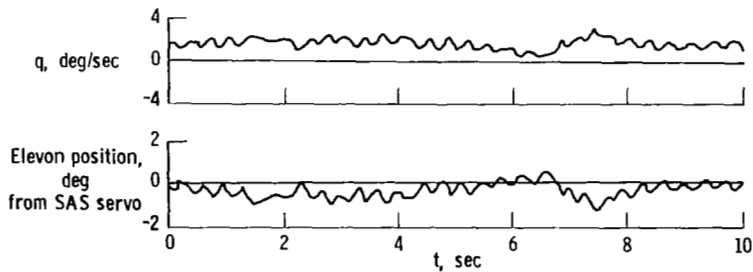
CORRELATION OF GROUND AND FLIGHT TEST RESULTS

Limit Cycle

Flight tests were made on the lifting body vehicles and the X-15 airplane to verify limit cycle characteristics predicted in ground tests. Figure 12(a) is a time history of pitch rate and elevon deflection during a severe pitch limit cycle oscillation on the first HL-10 lifting body flight. The pilot considered this oscillation to be objectionable



(a) Original SAS.



(b) Modified SAS.

Figure 12. Comparison of pitch limit cycle characteristics of the original and modified SAS of the HL-10 lifting body. $\bar{q} = 14,360 \text{ N/m}^2$ (300 lb/ft²); SAS gain = 0.3 deg/deg/sec.

primarily because of vehicle motion but partly because of control stick motion produced by surface rate limiting. Investigation showed that the pitch control power was higher in flight than had been predicted from wind-tunnel tests. Figure 12(b) shows that the limit cycle oscillation was reduced significantly after a notch filter and a lead-lag network were added to the system and all worn bearings and bushings were replaced. Figure 13 summarizes the limit cycle characteristics obtained in flight and ground tests of the original and the modified SAS.

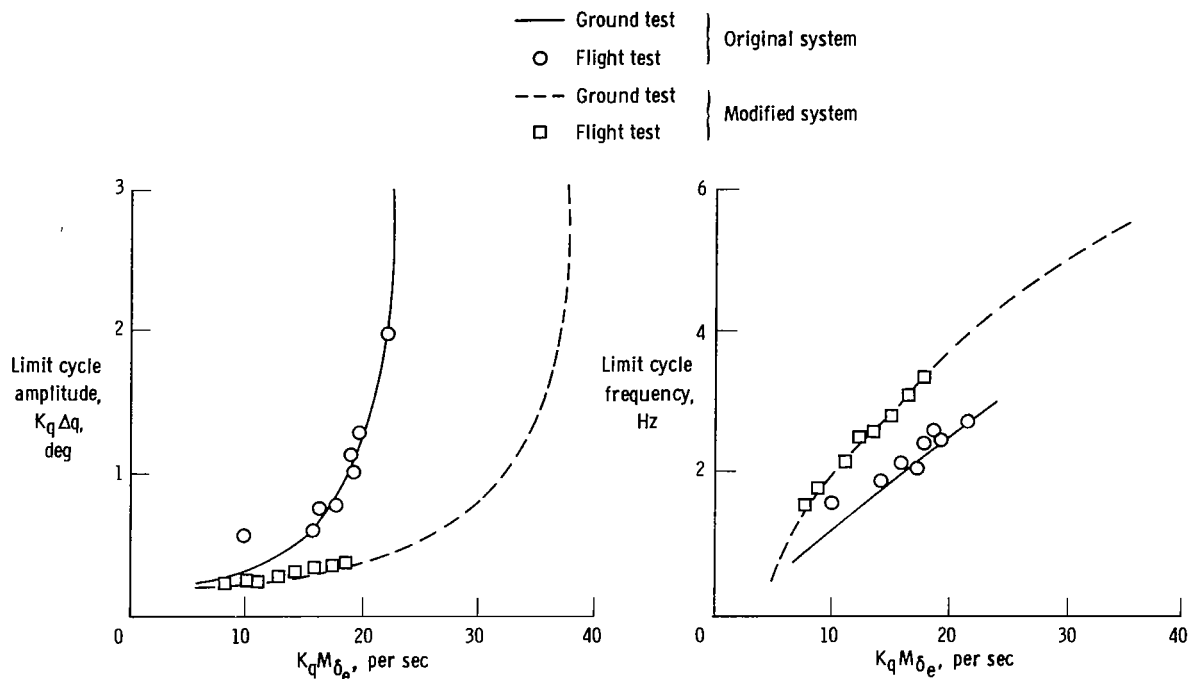


Figure 13. Summary of limit cycle test characteristics obtained from flight and ground tests of the original and modified pitch SAS of the HL-10 lifting body.

Figure 14 is a time history of roll rate and aileron deflection during a severe roll limit cycle oscillation on the X-15 airplane (refs. 1 and 2). The frequency of the limit cycle was about 3.2 hertz, and the amplitude was about 1° total change in bank angle.

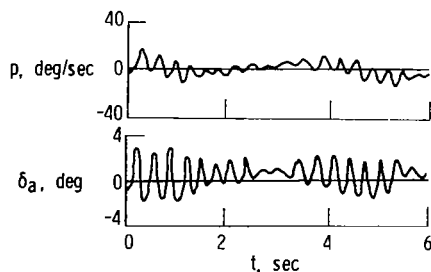
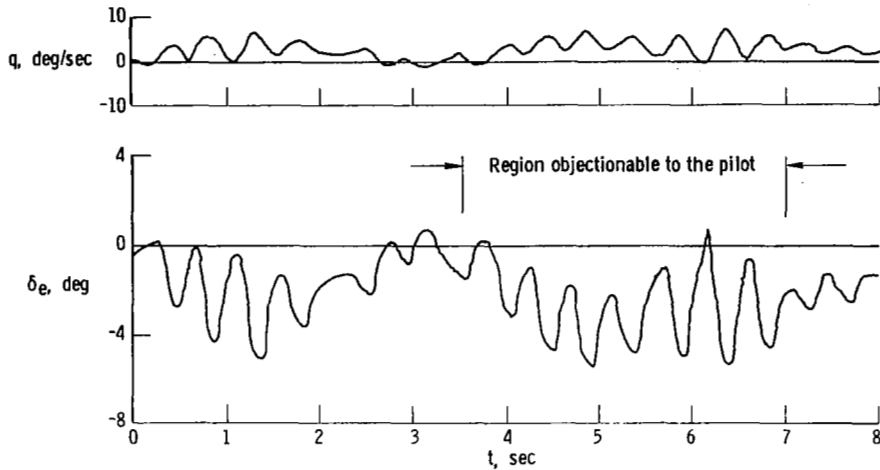


Figure 14. Time history of severe roll limit cycle oscillation of the roll SAS of the X-15 airplane.

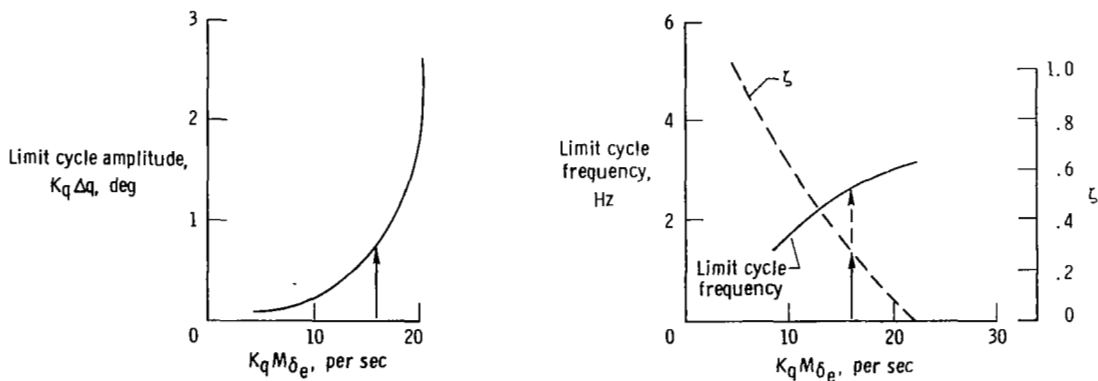
The pilot considered this oscillation to be objectionable because of the motion of the control stick caused by surface rate limiting. The amplitude of this limit cycle was not constant because of control input and a tendency to beat. The limit cycle was

reduced to an acceptable amplitude by modifying the SAS electronic filter.

Figure 15(a) is a plot of the pitch limit cycle characteristics that the pilot occasionally considered to be objectionable during an M2-F2 flight. The total loop gain, $K_q M_{\delta_e}$, was approximately 16 per second, at which the limit cycle amplitude, $K_q \Delta q$, is about 0.65° as shown in figure 15(b). This total loop gain also corresponds to a limit cycle damping factor of approximately 0.25.



(a) Flight test.



(b) Ground test.

Figure 15. Comparison of objectionable limit cycles from flight and ground tests of the M2-F2 lifting body.

Structural Resonance

During SAS ground tests before the first X-15 flight, it was possible to excite and sustain a 13-hertz system-airplane vibration in the pitch and roll axes. Thus a

second-order filter with a break frequency of 10 hertz was installed in the SAS. Although the modified filter reduced the roll limit cycle amplitude at the same frequency of 1 to 3 hertz, during ground tests it was possible to excite and sustain a system-airplane vibration at 13 hertz. A breadboard of the modified filter was flown at high damper gains, but the pilot failed to excite the vibration. During the rollout after touchdown, however, a severe vibration was experienced and the SAS had to be turned off. This led to the belief that the vibration would occur only on the ground. To prevent recurrence on the ground, a switch was incorporated in the airplane which automatically lowered the SAS gain to a safe level when the landing gear was extended. Five flights later, however, the vibration occurred during the reentry phase of a 51,000-meter (170,000-foot) altitude mission. Figure 16 is a time history of the vibration. A 13-hertz vibration is present in all the traces—left and right SAS links, left and right surface deflections, and roll rate. The pilot reported the vibration to be the most severe that he had ever encountered. The shaking was triggered by pilot inputs at low dynamic pressure (6220 N/m^2 (130 lb/ft^2)) and continued until the SAS gain was reduced slightly and dynamic pressure had increased to $47,880 \text{ N/m}^2$ (1000 lb/ft^2). Fortunately, the amplitude of the shaking was limited by rate limiting of the control surface actuators.

Because of the closed-loop nature of the problem, restrictions existed in the allowable gain at the structural frequencies. This is shown in figure 17 in which system gain is presented as a function of frequency for three filters, all at a SAS gain setting of 6.

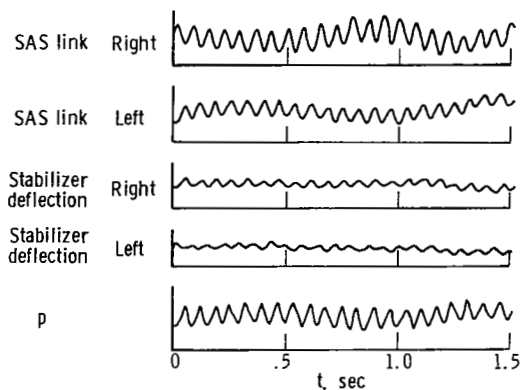


Figure 16. Time history of an in-flight vibration on the X-15 airplane (ref. 1).

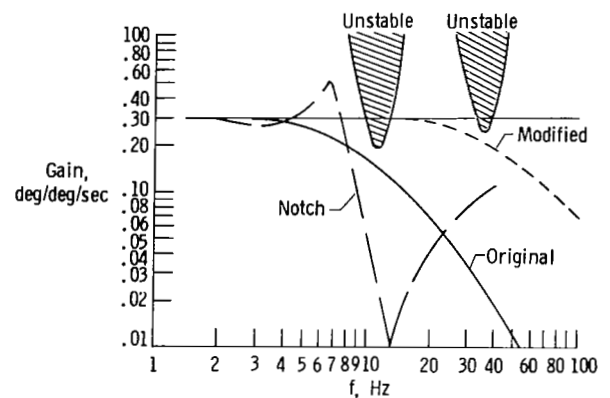


Figure 17. Effect of filters on high-frequency stability of the X-15 airplane (ref. 1).

If the curves intersect the boundaries which represent restrictions in gain at the structural frequencies of the horizontal tail at 13 hertz and 30 hertz, a sustained oscillation can occur. The modified filter used during the previously discussed altitude flight intersects the first boundary; a vibration, therefore, would be expected at 13 hertz. The original filter is free of the 13-hertz vibration, but produces unacceptable limit cycle characteristics at critical flight conditions. A notch filter circumvented both problems. This filter was designed to provide minimum phase lag at limit cycle frequencies and maximum filtering at the surface resonant frequencies.

Experience has shown that the structural damping of an aerodynamic surface may be altered by its aerodynamic environment. Figure 18 illustrates the effects of aerodynamic surface loading (proportional to indicated airspeed) on the SAS gain required to sustain a structural resonance.

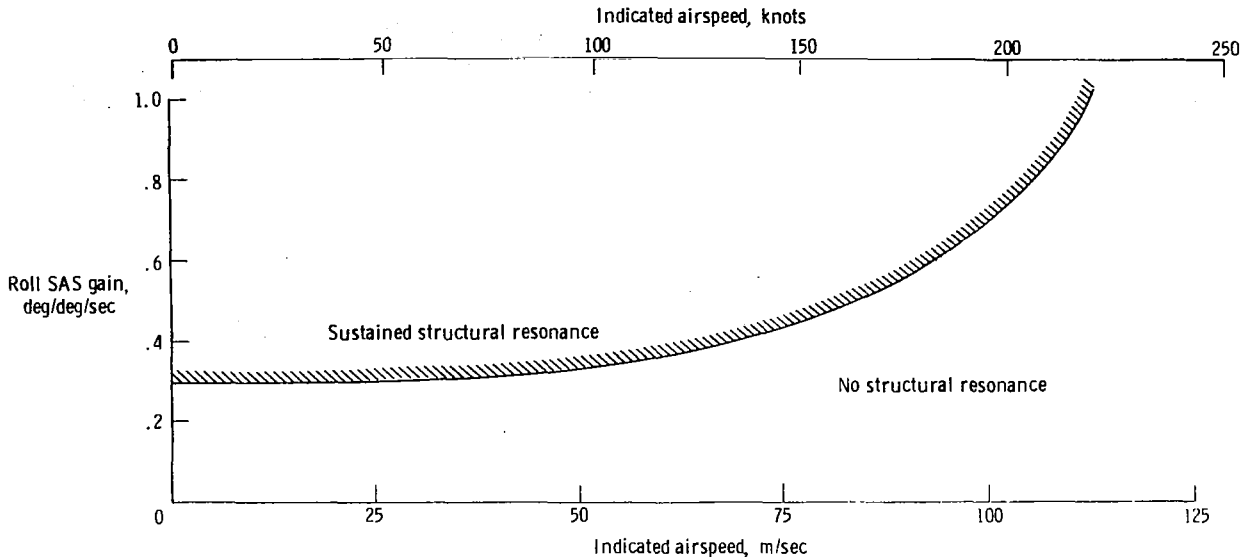


Figure 18. Typical results from structural resonance tests performed with the HL-10 lifting body mated to the launch airplane.

Structural resonance was encountered also on a fighter-type airplane flying with a fixed SAS gain. As fuel loading decreased, the structural resonance occurred; thus a reduction in SAS gain alleviated the problem.

The problems of structural resonance and limit cycle must be approached simultaneously because improvement in one will result in degradation of the other.

Criteria for Flight Acceptance

Limit cycle.—The amplitude of a steady-state limit cycle is a good indication of the proximity of the limit cycle to the point where the system diverges and of how much it will annoy the pilot. Flight limit cycle data were processed in terms of limit cycle amplitude versus combinations of control power and SAS gain and correlated with pilot evaluations of the limit cycle phenomenon and ground test data. As a result of the data analysis, a conservative limit cycle criterion was established in terms of ground test data for the lifting body vehicles and the X-15 airplane. The criterion was applied during preflight checks to preclude the occurrence of objectionable limit cycles in flight and to insure flight safety. The criterion is: The limit cycle amplitude (SAS gain multiplied by peak-to-peak angular rate) shall not exceed 0.5° for the highest product of control power and SAS gain that will be used in flight.

It should be noted that a limit cycle amplitude of 0.5° may produce a control surface oscillation which is barely detectable during ground test. In flight, however, for the same value of loop gain, the damping characteristics of the system permit transient oscillations to be two to three times as large as the steady-state limit cycle oscillations because of disturbances produced by pilot control inputs and atmospheric turbulence.

Nevertheless, this increase in amplitude has been acceptable.

The limit cycle criterion for ground tests was based on the summary plot shown in figure 19, which was generated from pilot evaluations and flight data from several research vehicles. In the acceptable region, limit cycles are unnoticed by the pilot in flight and cause no difficulty in controlling the vehicle. In the marginal region, they

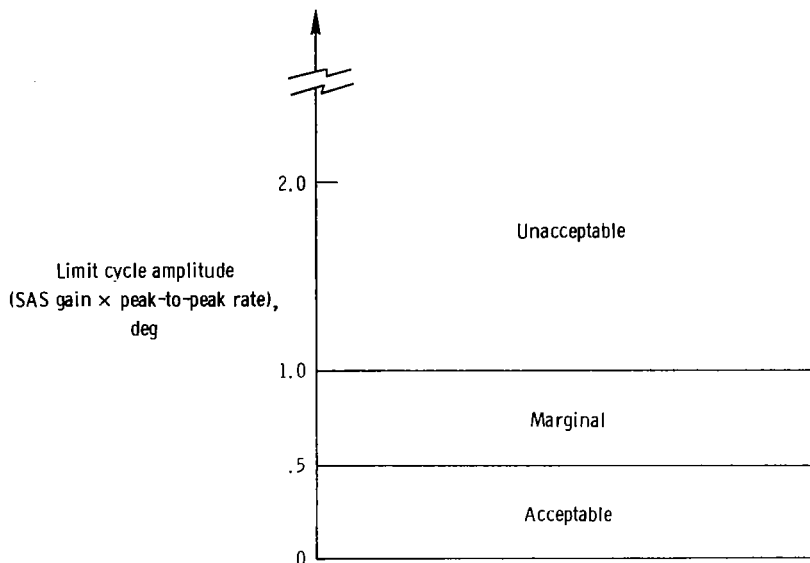


Figure 19. Summary rating scale of limit cycle characteristics, based on pilot evaluations and flight data from several research vehicles.

are detected by the pilot and decrease the controllability of the vehicle for precise maneuvers. The pilot feels the acceleration and may sometimes believe that it is buffet and that he may lose control of the vehicle. The limit cycles in the unacceptable region can cause the pilot to lose control of the vehicle. The destructive region begins where aerodynamic loads approach the structural limitation of the vehicle and continues until the structure fails.

Because any change in a rate feedback loop alters limit cycle characteristics, it is important to satisfy the structural resonance criterion before the final limit cycle tests are performed. In general, an improvement in either limit cycle or structural resonance will result in degradation of the other. Thus these two problems must be approached simultaneously. To achieve the highest possible total loop gains, some combination of lead-lag networks and notch filters is usually required in the control system electronics.

Structural resonance.—Data from structural resonances which occurred during flights of several research vehicles were recorded and compared with ground test data. To set limit cycle standards, the following criterion for minimizing structural resonance was established: The maximum in-flight SAS gain should never exceed 50 percent of the value at which a structural resonance can be sustained during ground test.

CONCLUSIONS

Ground and flight test limit cycle and structural resonance experience with the stability augmentation systems (SAS) of three lifting body vehicles and the X-15 airplane led to the following conclusions:

1. Limit cycle and structural resonance problems must be approached simultaneously because any improvement in one will result in a degradation of the other.

2. In limit cycle tests the position transducer must be located on the actual control surface.

3. A ground test criterion for predicting objectionable limit cycle oscillations in flight is: The limit cycle amplitude (SAS gain multiplied by peak-to-peak angular rate) shall not exceed 0.5° for the highest product of control power and SAS gain that will be used in flight.

4. A ground test criterion suitable for minimizing structural resonance is: The maximum in-flight SAS gain should never exceed 50 percent of the value at which a structural resonance can be sustained during ground test.

5. Primary consideration in the design of a stability augmentation system should be the location of the sensors and the SAS servos.

Flight Research Center,
National Aeronautics and Space Administration,
Edwards, Calif., January 10, 1972.

REFERENCES

1. Taylor, Lawrence W., Jr.; and Merrick, George B.: X-15 Airplane Stability Augmentation System. NASA TN D-1157, 1962.
2. Taylor, Lawrence W., Jr.; and Smith, John W.: An Analysis of the Limit-Cycle and Structural-Resonance Characteristics of the X-15 Stability Augmentation System. NASA TN D-4287, 1967.
3. Stambler, Irwin: Manned Maneuverable Reentry. Space/Aeronautics, vol. 41, no. 5, May 1964, pp. 44-52.
4. Thompson, Milton O.; Peterson, Bruce A.; and Gentry, Jerauld R.: Lifting-Body Flight Test Program. SETP Technical Review, second 1966 issue, vol. 8, no. 2, Sept. 1966, pp. 1-22.
5. Holleman, Euclid C.: Stability and Control Characteristics of the M2-F2 Lifting Body Measured During 16 Glide Flights. NASA TM X-1593, 1968.
6. Painter, Weneth D.; and Kock, Berwin M.: Operational Experiences and Characteristics of the M2-F2 Lifting Body Flight Control System. NASA TM X-1809, 1969.
7. Rickard, Richard R.; and Gentry, Jerauld R.: Development Testing of a High-Gain Adaptive Control Augmentation System Installed in an F-4C Aircraft. Volumes I and II. FTC-TR-TD-70-4, Air Force Flight Test Center, Edwards Air Force Base, Calif., Sept. 1970.
8. Kotfila, Ronald P.; and Painter, Weneth D.: Design, Development, and Flight Test Experience With Lifting Body Stability Augmentation Systems. AIAA Paper 69-887, 1969.
9. Mechtly, E. A.: The International System of Units - Physical Constants and Conversion Factors. NASA SP-7012, 1969.